Mechanical properties, EDM process optimization, and wear performance of Al 7075-based NiCr-graphite reinforced metal matrix composites

R. Palani[1*], S. Ilaiyavel[2], Mathanbabu Mariappan[3]

[1]*Department of Mechanical Engineering, Vel Tech High Tech Dr. Rangarajan Dr. Sakunthala Engineering College, Chennai, Tamil Nadu, 600062, India*
[2]*Department of Mechanical Engineering, Sri Venkateswara College of Engineering, Pennalur, Sriperumbudur, Chennai-602 117, India*
[3]*Department of Mechanical Engineering, Government College of Engineering, Bargur, Krishnagiri, Tamilnadu-635104, India*

Aluminum matrix composites are increasingly popular in the automobile and aerospace sectors due to their enhanced stiffness, low weight, and high strength. This study aims to enhance the quality of aluminum metal matrix composites by incorporating nickel, chromium, and graphite using the stir casting method. The influence of varying proportions of nickel, chromium, and graphite on the material's behavior was analyzed by altering the reinforcement composition. The mechanical properties of the composite were assessed through tensile, impact, and hardness testing. The machining characteristics in wire electrical discharge machining (WEDM) were optimized using the Taguchi method across various parameters. Wear analysis of wire-cut specimens was conducted using a pin-on-disc apparatus. Results indicated that the specimen with 4% graphite and 10% nickel-chromium exhibited superior mechanical properties and wear resistance compared to other specimens. Optimization results revealed that a material removal rate (MRR) of 0.055978 g/min and a surface roughness (SR) of 3.2 µm were achieved with input parameters of 50 V, 6 A current, 6 µs pulse-on time, and 14 µs pulse-off time in WEDM, resulting in a smooth surface finish. Post-wear microstructural evaluation was conducted using scanning electron microscopy (SEM); energy dispersive spectroscopy (EDS) was employed to analyze the elemental distribution within the material. EDS analysis confirmed a uniform distribution of reinforcement materials throughout the composite.

Keywords: Aluminum metal matrix, optimization, wear, machining parameters, SEM, EDS

INTRODUCTION

Composites are materials with phases that are dissimilar, with a distinct surface separating them. They exhibit extraordinary mechanical and thermal properties and find large applications in the field of material science [1]. Ceramics, metals, and polymers may be utilized as matrices for composites. Metal matrix composites are formed when a metal is used as the matrix or supporting structure. A metal matrix is made up of two phases: one that serves as a supporting framework and the other that serves as a disseminated phase [2]. Aluminum is one of the engineering materials with high strength utilized extensively for structural applications. Aluminum composites possess excellent properties compared to pure aluminum or alloys of aluminum [3]. The making of metal matrix composites (MMC) can be done using many methods like powder metallurgy, stir casting under friction, hot forging, stir casting and squeeze casting [4]. Stir casting is a commonly utilized method for fabrication of metal matrix composites [5]. Nickel,

chromium and graphite showcase good tribological properties, so they are used mostly for reinforcing with metal matrix in which there is chance of wear [6]. The graphite in the MMC acts as a self-lubricating medium which in turn lowers the rate of wear [7]. Metal matrix composites embedded with ideal material in it are unique and have tremendous opportunity in design of special components in the automotive field [8].

Research is going on in the field of material engineering to produce materials with good qualities. A lot of researchers have contributed to material science by using aluminum as the metal matrix for their reinforced composites using various materials for reinforcement. Madeva Nagaral *et al.* [9] used stir casting to create an Al7475 metal matrix supplemented with 5% wt. of nano Al_2O_3. According to ASTM standards, it was tested for hardness, ultimate yield strength, and elongation. The wear analysis was done using a pin-on-disc device experiment with stable speed and variable weights. Bharath *et al.* [10] used the unique notion of two-step reinforcements in the stir casting method

* To whom all correspondence should be sent:
E-mail: *rpalani456@gmail.com,*
palani@velhightech.com

to manufacture Al_2O_{14} with Al_2O_3 ceramic. SEM and microstructure analyses indicated that the Al_2O_3 distribution was quite uniform. The wear rate identified by particle refinement was determined using XRD spectroscopy. Experimentation reveals that the optimal mixer combinations resulted in a hardness of 68.54 percent (15 wt. percent) and a tensile strength of 29.03 percent (15 wt. percent). Greater wear resistance qualities were obtained from the composites, and worn surfaces were investigated by SEM analysis.

Han *et al.* [11] indicated that the machining of MMC is difficult due to the difference in properties between the metal matrix and reinforced materials. An experimental investigation was done to evaluate the impact of process factors responsible for machining metal matrix on the final surface finish. The results indicated that selecting optimized parameters is paramount for producing a finished and smooth surface. Palaniswamy *et al.* [12] experimentally studied and optimized aluminum MMC. The machine factors, like discharge current and pulse timing, were optimized to improve the metal removal rate and reduce the rate of tool wear. The findings of the study show that the discharge current is an important parameter in governing the surface finish produced.

In the current work, Al7075 is employed as the base material which is stir-cast with Ni-Cr and graphite. The addition of Ni-Cr improves the properties of the MMC, which directly influences its ability to withstand abrasive forces and reduces the wear rate. Graphite, known for its solid lubricating properties, helps in decreasing the coefficient of friction, thereby reducing wear and improving the machinability of the composite. The improved hardness by Ni-Cr and the lubrication by graphite systematically contribute to the superior wear resistance and durability of the composite. The combination of materials utilized for MMC is not used so far in the literature for making MMC out of aluminum. The distinguishing feature of the present study is optimization of EDM-machining characteristics of the novel MMC with wear and mechanical characteristics.

EXPERIMENTAL

The fabrication and characterization are done in five phases: fabrication, mechanical testing, EDM machining optimization and wear test followed by morphological analysis. The basic material is an Al7075 polished rod shown in Figure 1. The needed amount of Al7075 is cut from the raw material, cleaned, and accurately weighed before casting. Ni-Cr and graphite are taken in the form of powder. The

fabrication of aluminum metal matrix reinforced with Ni-Cr and graphite follows the steps: mold preparation, raw materials melting using the stir casting method followed by pouring into the mold cavity and finally machining the cast aluminum metal matrix for testing. The different composition percentage fractions of Al7075 reinforced with Ni-Cr and graphite utilized to make three specimens are given in Table 1.

Table 1. Al7075, Ni-Cr and graphite proportions

Specimen	Al7075 %	Ni-Cr %	Graphite %
1 (A)	93	5	2
2 (B)	86	10	4
3 (C)	79	15	6

Mold preparation

A wooden pattern is made depending on the required specimen dimensions. The area between the pattern and the mold box is filled with sand, finer sand inside (facing sand) and coarser sand outside (backing sand). The pattern is carefully removed so that no harm is done to the mold cavity (Figure 1).

Figure 1. Aluminum base material and mold

Stir casting

The main process involved in MMC fabrication is stir casting, which is the most commonly used method due to its simplicity and viability [13]. The stir casting device, shown in Figure 3, was utilised for melting the ingredients. It is constructed from a conical graphite crucible that can hold on heat up to 680°C. The crucible is put in the alumina ceramic muffle. The heating element Kanthol-A1 is wrapped around the muffle. This furnace uses resistance heating. To avoid oxidation, the stirring operation is done in an enclosed steel chamber filled with nitrogen and inert gas. The current temperature of the liquid is measured using a K-type thermocouple with a working temperature of -200°C to 1250°C. EN24 is a stirrer shaft material that is resistant to corrosion. One end of the shaft is connected to a 0.5 hp PMDC motor through a flange connection. Four blades are fused at the opposite end of the shaft at 45°C. To minimise particle coagulation and segregation when employing a hopper, a consistent feeding rate of reinforcement particles is essential.

The polished Al7075 rod is heated in the furnace. The molten matrix is swirled gently at 30 rpm, then the rate raised to 300-600 rpm using a speed controller. A combination of Ni-Cr and graphite is

as shown integrated into the MMC at a semisolid level at 640°C for a scattering duration of 5 min. The mixture is then warmed above the melting point temperature before being poured into the mold. The composite slurry in molten state is then poured into the rectangular sand mold.

Then, the Al7075 composite material which is rectangular in shape, is prepared in Figure 2. The composite material is separated and cut into pieces by a milling machine after it has cooled and taken out from the mold, as shown in Figure 2 (c).
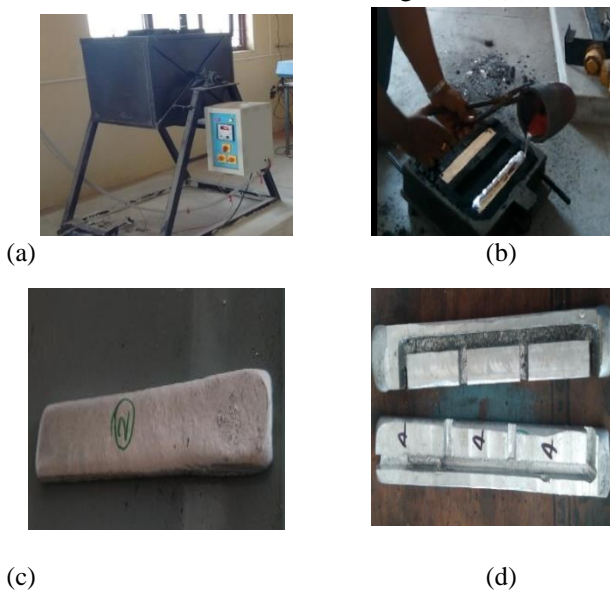
Figure 2. (a) Stir casting apparatus, (b) Pouring process, (c) Al 7075 composite test bar and (d) Al 7075 composite material after milling.

Mechanical testing

Rockwell hardness tester was utilized for testing the hardness of the obtained metal matrix composite. An indenter with a ball of 2.5 mm diameter at a pressure of 500 N pressure is used for hardness testing [14]. ASTM B-557 is followed for carrying out a tensile test [15]. Charpy impact test is used to study the load absorption capability of the MMC. ASTM E23 is followed for carrying out an impact test [16].

Wire cut electrical discharge machine (WEDM)

The wire cut EDM machine of CNC is utilized for machining the specimens. The model's name of the machine is YCM W350. The machining is done by a thin electric wire in which the tool acts as an electrode and a dielectric fluid is passed between the tool and work piece, which carries away the vaporized or moisturized debris coming from the

machining [17]. The wire cut EDM process was carried out on three specimens of various proportions. The specimens of the novel metal matrix composite (MMC) used for WEDM are shown in Figure 3.

(a) MMC A (b) MMC B (c) MMC C
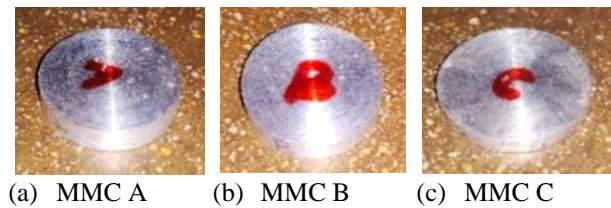
Figure 3. (a-c) Metal matrix composites used for EDM.

Optimization of WEDM by the Taguchi method

Taguchi method is an optimization technique which helps in identifying the impact of the parameters involved in the experiment on the mean and variance of a particular process output. This type of optimization will reduce the experimentation work and the cost involved. The performance of the system is analyzed using signal-to-noise ratio (S/N) which is defined as the ratio between the desired value to the undesired value [18]. The input parameters of the wire cut electrical discharge machine, such as current, pulse-on time, voltage, pulse-off time were optimized to get the output parameters material removal rate (MRR) and surface roughness (SR). Taguchi method is utilized in expert design optimization [19, 20]. For obtaining the optimized parameters, the levels of process parameters involved in WEDM are initially set. The set levels of process parameters [21] are presented in Table 2.

Table 2. EDM process parameters

Parameters	1	2	3
Peak current	7	11	13
Servo voltage	54	51	51
Pulse-on time	3	2	5
Pulse-off time	21	20	16

Wear testing

Wear testing is done on the specimens machined using wire cut EDM. The pin-on-disc method ASTM designation G99 procedure is used as a standard procedure to acquire the wear results from specimens [22]. The pin-on-disc apparatus used has a load carrying capacity up to 60 N, rotational speed 500 N, frictional force up to 20 N and compound wear up to 1200 μm.

Table 3. Input parameters for optimization

Exp. No.	Current (A)	Voltage (V)	Pulse-on Time (µs)	Pulse-off Time (µs)
1	8	55	2	20
2	8	53	3	19
3	8	52	4	17
4	10	55	3	17
5	10	53	4	20
6	10	52	2	19
7	12	55	4	19
8	12	53	2	17
9	12	52	3	20

The typical pin specimen is cylindrical in shape. The diameter and the thickness of the disc specimen range from 30 to 100 mm and 2 to 10 mm, respectively. Before testing, the specimen is cleaned and dried with non-chlorinated, non-film-forming cleaning chemicals and solvents. Drying removes the residues of fluids entrapped in the material during cleaning. Steel (ferromagnetic) specimens that have residual magnetism are also demagnetized. The weight of the specimens measured is appropriately around 0.0001 g. To maintain the proper contact conditions, the pin-shaped specimen is carefully placed in its holder and adjusted so that it is perpendicular (61° degree) to the disc surface when in contact. A mass of 2 kg is added to the system lever to force the pin against the disc. The motor is started and set to a speed of 300 rpm while keeping the pin specimen away from the disc. The specimen is weighed before the testing using a weighing scale. Then it is brought in contact with the disc under load. After 10 min, the test is terminated. Tests should not be paused or resumed. The specimen is removed and cleaned, and the surface is examined for protrusions, displaced metal, discoloration, micro cracking, and spots. To acquire statistically significant findings, the specimen is measured again and the test is repeated with multiple specimens. The pin-on-disc experiment parameters are tabulated in Table 4.

Table 4. Pin-on-disc apparatus parameters

Parameters	Value	Unit
Force	2	kg
Speed	300	rpm
Duration	10	min

Morphology

Surface morphology of the specimens which have been subject to wear, were studied using SEM and EDS. SEM helps in identifying the surface defects encountered after the specimen have been subject to wear. EDS is utilized for identifying the

presence of reinforcement added to the aluminum metal. The amount of reinforcement present in the final material can be easily identified by XRD patterns observed during EDS analysis [23].

RESULTS AND DISCUSSION

Mechanical characteristics

Hardness is the property which helps the MMC in withstanding the surface wear and tear. As the hardness of the MMC increases, the property of the MMC to withstand wear also increases. The presence of chromium and nickel along with graphite have improved the hardness of the composite. Especially nickel provides an additional hardening effect [24].
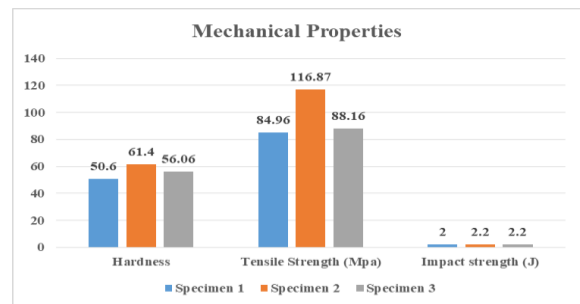
Figure 4. Mechanical strength of MMC

Specimen 2 shows the highest hardness among all specimens. The results of tensile and impact test also show that the performance of specimen 3 is best with 116.16 MPa of tensile strength and 2.2 J of impact strength. The improved tensile strength is due to the presence of graphite [25].

Machining characters

- *Rate of material removal and surface finish*

The rate of material removal is directly proportional to the weight difference between initial specimen before machining (WBM) and final specimen after machining (WAM), and inversely proportional to the machining time (MT).

Material removal rate = WBM – WAM / MT

Surface roughness (SR) indicates the texture. Surface roughness can cause irregular surface which will be easily corroded. If the surface layer is substantial, the surface will become rough; if the surface variations are minor, the surface will be smooth. Surface roughness is measured with a profile gauge. The minimal surface roughness value is for specimen 3 - 3.2 µm. The greatest surface roughness value is for specimen 2 - 6.6 µm, as shown in Table 5. Table 5 shows that 4 of the 9 specimens had higher surface roughness values calibrated using a surface profile gauge.

Table 5. Material removal rate (MRR) and surface roughness (SR)

Exp. No.	WBM (g)	WAM (g)	MT (min)	MRR (g/min)	SR (µm)
1	17.2955	17.0336	5.25	0.049885	3.4
2	17.6479	17.3934	5.66	0.044964	6.6
3	19.1614	18.8606	5.33	0.055978	3.2
4	17.6483	17.3766	5.08	0.053484	6.2
5	17.2082	16.9372	5.03	0.053876	3.8
6	18.0875	17.7942	5.16	0.056841	5.6
7	17.2947	17.0086	4.93	0.058032	3.9
8	18.5701	18.2610	5.65	0.054707	6.5
9	17.4121	17.1202	4.65	0.062774	5.0

Table 6. Input parameters and output parameters

Exp. No.	Input parameters				Output parameters	
	Machining parameters (WEDM)					
	Current (A)	Voltage (V)	Pulse -on Time (µs)	Pulse -off Time (µs)	MRR(g/min)	SR(µm)
1	8	55	2	20	0.049885	3.4
2	8	53	3	19	0.044964	6.6
3	8	52	4	17	0.055978	3.2
4	10	55	3	17	0.053484	6.2
5	10	53	4	20	0.053876	3.8
6	10	52	2	19	0.056841	5.6
7	12	55	4	19	0.058032	3.9
8	12	53	2	17	0.054707	6.5
9	12	52	3	20	0.062774	5.0

Table 7. Output response for MRR and SR

Response for MRR				
Level	Current	Voltage	Pulse-on Time	Pulse-off Time
1	0.04985	0.05789	0.05247	0.05244
2	0.05372	0.05102	0.05289	0.05216
3	0.05960	0.05270	0.05465	0.05681
Delta	0.00790	0.00650	0.00225	0.00215
Rank	1	2	3	4
Response for SR				
Level	Current	Voltage	Pulse-on Time	Pulse-off Time
1	4.326	4.394	4.992	5.112
2	5.231	4.987	5.223	4.936
3	5.102	4.365	3.564	4.326
Delta	0.675	1.32	2.356	1.289
Rank	4	3	1	2

Table 8. Signal-to-noise ratio

Exp. No.	MRR		SR	
	S/N Ratio	Mean	S/N Ratio	Mean
1	-25.0982	0.045691	10.6296	3.4
2	-26.9427	0.044964	16.3909	6.6
3	-24.9690	0.056435	10.3703	3.3
4	-25.4355	0.053484	15.8478	6.2
5	-25.3721	0.053876	11.5957	3.8
6	-24.9068	0.056841	14.9638	5.6
7	-24.7266	0.058032	11.8213	3.9
8	-25.2391	0.054707	16.2583	6.5
9	-24.0444	0.062774	13.9794	5.0

(a)

(b)

(c)

(d)
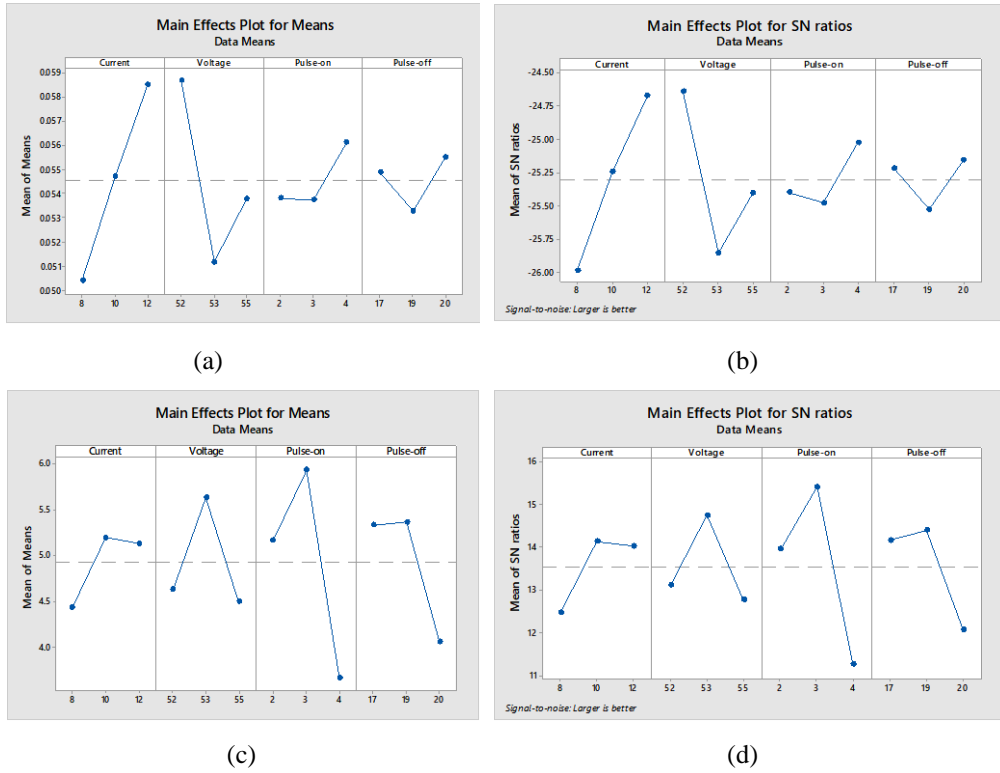
Figure 5. (a-d) Mean effect plots

(a)

(b)
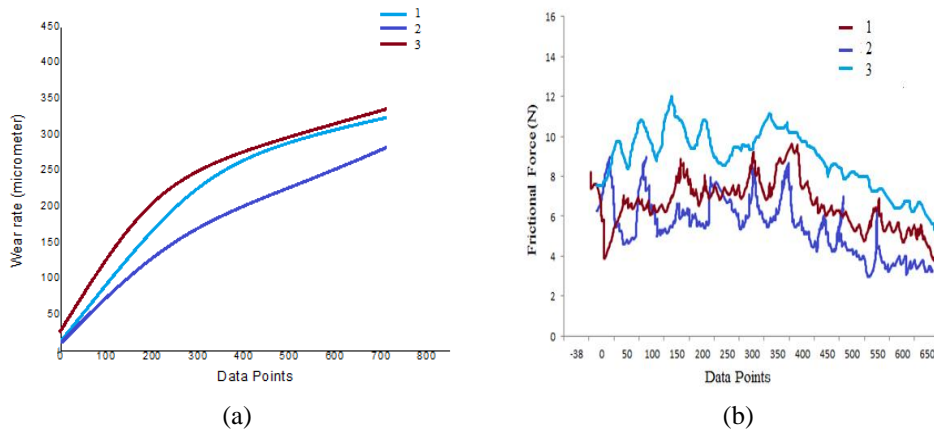
Figure 6. (a and b) Wear in μm and friction force in N, for MMC of various proportions

Analysis of MRR and SR

Surge in pulse-on time leads to a surge in discharge energy, resulting in stronger explosions and higher MRR [26]. Increased cutting speed leads to greater surface roughness [27]. Surge in pulse-on duration and peak current result in more electrons hitting the work surface, causing greater material erosion per discharge. Table 6 shows the input parameters and output parameters.

Table 7 shows the mean responses for material removed and surface roughness based on input parameters of WEDM. From the results obtained it is clear that the discharge current has an important impact on the finish of the surface obtained and the rate of material removal of the specimen.

The plot of means is shown in Figure 10. The mean of effect plots help in identifying the impact of a particular process parameter on the output response (MRR and SR) [28]. From the graph it is clear that both current and voltage impact the MRR. Pulse-on time and pulse-off time impact the surface finish. The lower the S/N ratio, the parameters are most suited. From the table it is clear that the parameters used in the third experiment show the lowest S/N ratio, which shows that the third set of parameters is the optimal one.

Wear analysis

The weight loss due to wear of Al7075/Ni-

Cr/graphite composite is calculated by using the difference in weight loss before experiment to weight loss after experiment. Weights of the pieces range from 10.49 to 11.11 g. The resistance to wear of the composite altered when the percentages of reinforcements were adjusted. Figure 6 (a) depicts the findings of wear rate in μm. The specimen 3 with 6 % graphite and 15 % nickel-chromium content, has the worst wear resistance. When the graphite proportion steeps, the specimen becomes more ductile and the composite's resistance to wear decreases. This is because addition of graphite leads to an increase in the Van der Waals forces between the particles, which will weaken the surface [29].

Test specimen 2 contains 4 % graphite and 10 % nickel-chromium and has a higher wear resistance. The nickel-chromium combination reduces the dislocation which increases the wear resistance. As the nickel-chromium content increases, the material's hardness improves, resulting in improved wear resistance [30]. The addition of graphite in a low amount will help self-lubricating the material and thereby improving the wear characteristics [31].

The friction force observed for the specimens is shown in Figure 6 (b). The higher friction force will simultaneously lead to a higher wear rate. For specimen 2, the friction factor is very low in comparison to the other specimens. The lower friction of specimen 2 is due to the strong bonding at the interface of the material while in specimen 3, the friction force is in an upward trend due to the weak inter-bonding at the interface of the material. This consequently leads to a higher frictional force and an increased wear rate.

Figure 7 depicts the wear rate for specimens of different proportions. The graph depicts the weight reduction (g) after the specimens have been subjected to wear test.
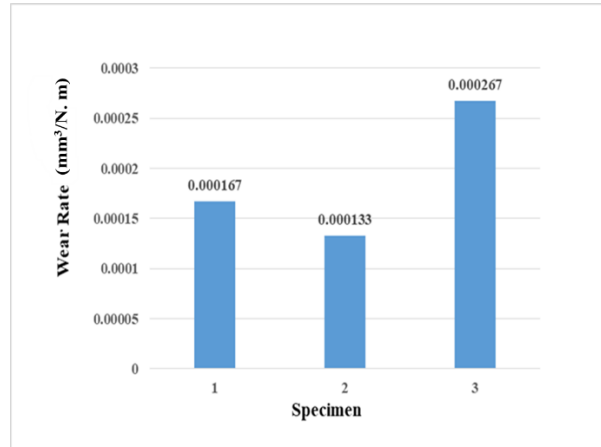
Figure 7. Wear test data comparison

Scanning electron microscopy (SEM) analysis

Figures 8-10 show the surface morphology image of the test specimens at different magnifications. It was revealed from the specimen SEM images, as shown in Figure 8 for specimen 1, that some parts of the specimen had crack development, which leads to a brittle fracture. The worn-out area of the surface indicates that its microstructure had fracture propagation. Lumps are also seen, which may be due to the clustering during reinforcement [32, 33].

The test specimen 2 was examined by scanning electron microscopy at magnifications of 10, 20, 50, and 100 m, as shown in Figure 9, and it was discovered that some parts of the specimen had a portion of fused particles, patches, grooves, and crack formation in a smaller amount. This is due to the less brittle structure due to the presence of 10 % Ni-Cr and the addition of 4 % graphite in the mixture. These factors resulted in a less wear character.
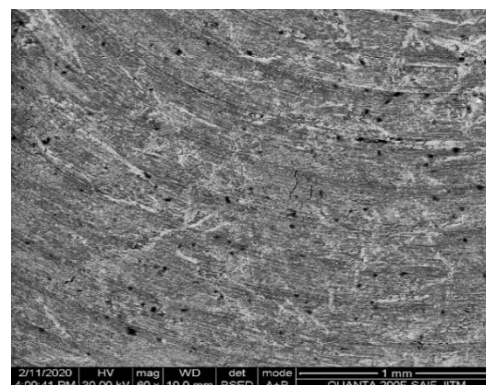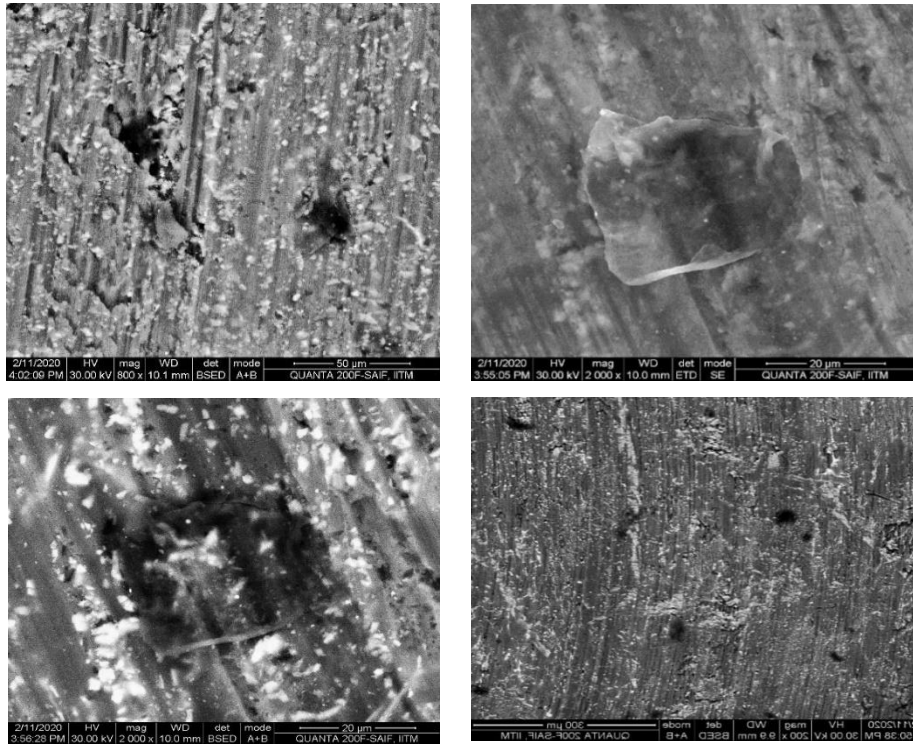
Figure 8. Specimen "1" SEM image analysis at various magnifications
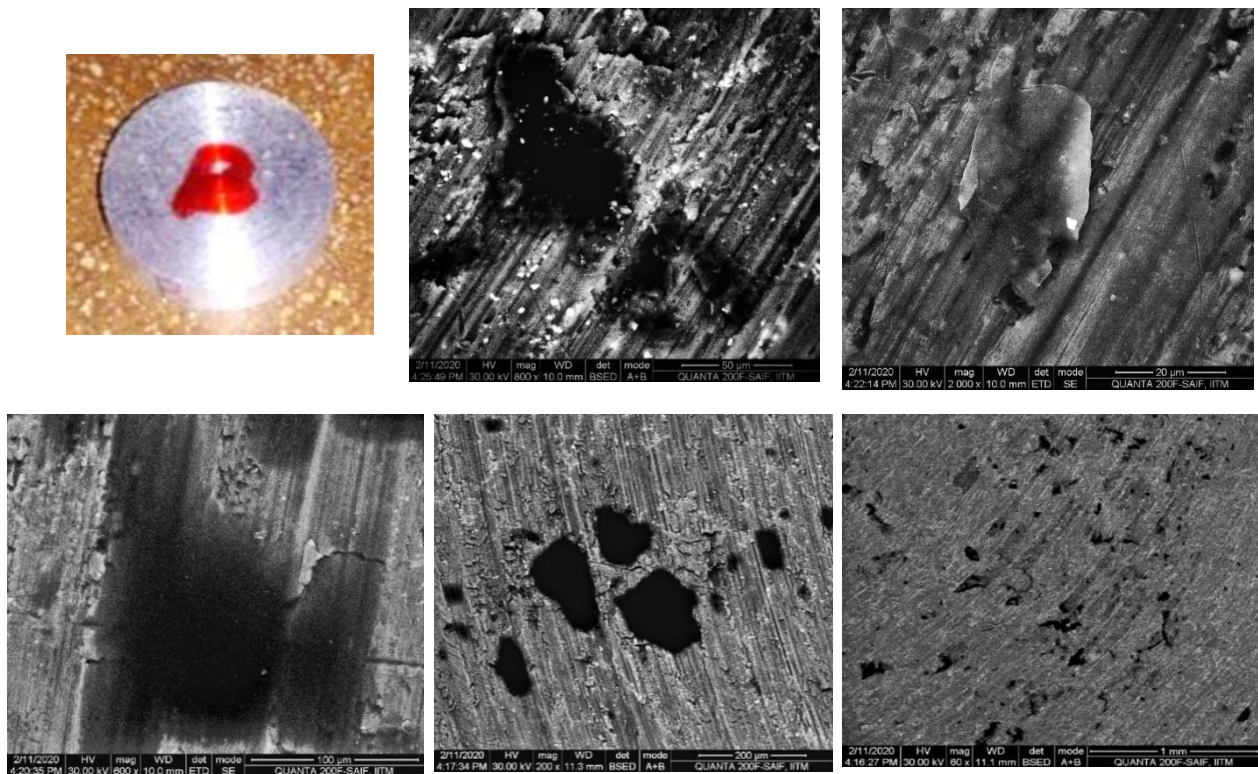
Figure 9. Specimen "2" SEM image analysis at various magnifications
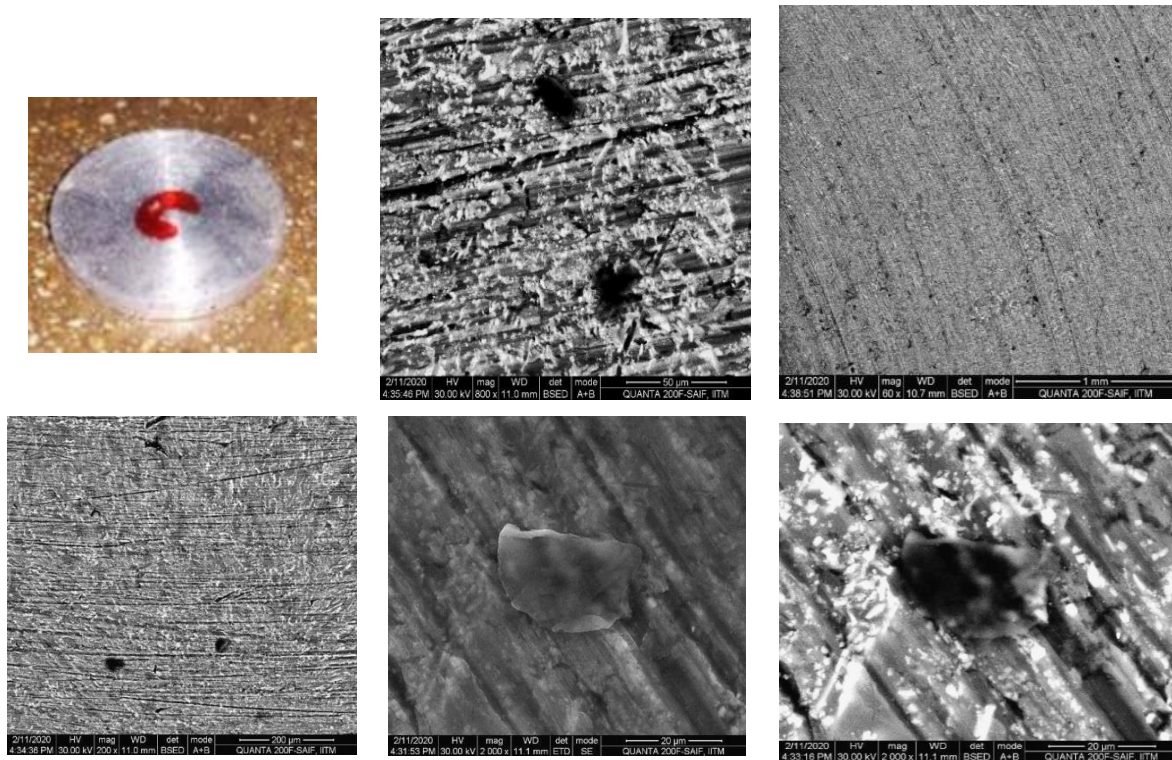
Figure 10. Specimen "3" SEM image analysis at various magnifications
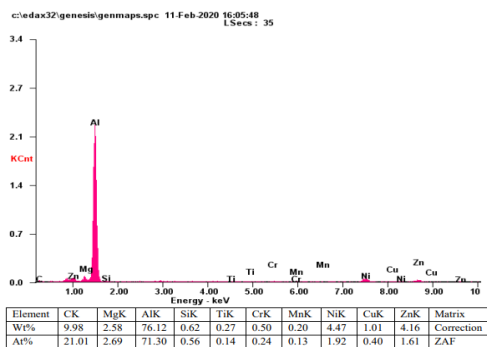
(a) EDS spectrum of specimen 1
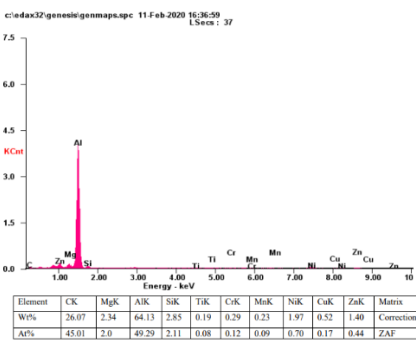
(b) EDS spectrum of specimen 2
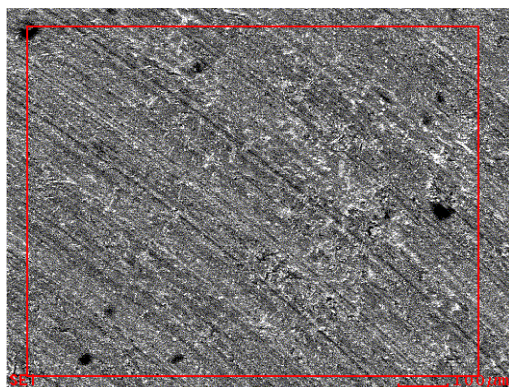
(c) EDS image of specimen 1

(d) EDS image of specimen 2

(e) EDS spectrum of specimen 3
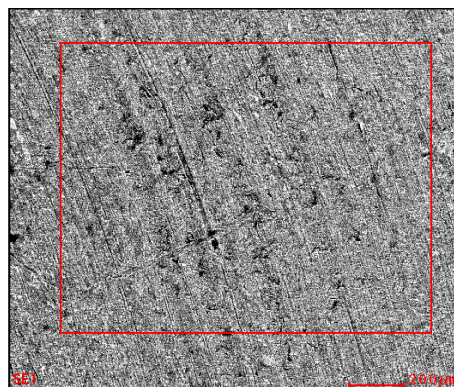
(f) EDS image of specimen 3
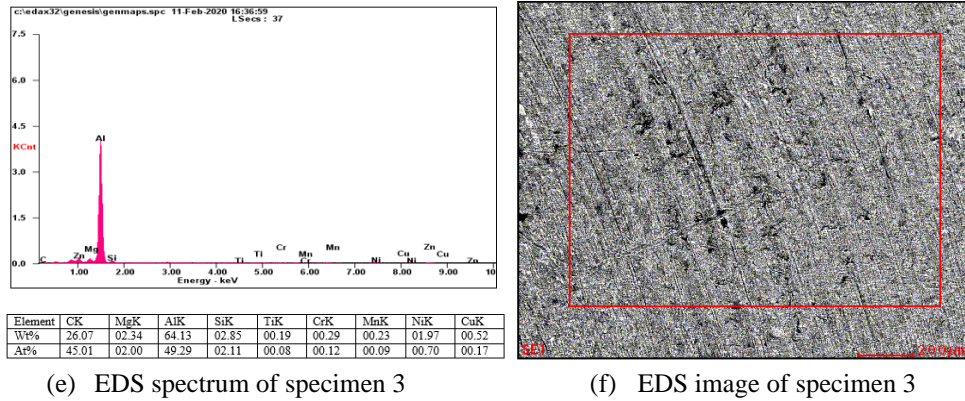
Figure 11. (a-f): EDS spectra and images obtained for MMC of various proportions

Element	CK	MgK	AlK	SiK	TiK	CrK	MnK	NiK	CuK
Wt%	26.07	02.34	64.13	02.85	00.19	00.29	00.23	01.97	00.52
At%	45.01	02.00	49.29	02.11	00.08	00.12	00.09	00.70	00.17

EDS analysis

The graphs showing the dispersion of energy through-out are presented in Figure 11. The concentration of all reinforced materials is presented in the EDS spectra. The presence of nickel, chromium and graphite peaks is clearly visible in the EDS spectra. From the quantitative table of EDS spectra, it is seen that the metal matrix phase of aluminum is dominant with highest percentage in terms of weight.

CONCLUSIONS

An Al7075/Ni-Cr/graphite composite material was successfully fabricated using the stir casting process. Mechanical testing of the MMC was conducted, revealing satisfactory tensile strength, hardness, and impact strength values. The pin-on-disc apparatus was used to evaluate different stir-cast specimen combinations, with wear results calculated based on the weight difference of specimens before and after testing. The wear characteristics and mechanical properties of the Al7075/Ni-Cr/graphite composite were analyzed, with findings indicating that the composite containing 4% graphite and 10% nickel-chromium outperformed other material combinations. The machining behavior of the MMC in WEDM was optimized using the Taguchi method prior to wear testing. The optimization revealed that current and voltage significantly impact output parameters such as surface finish and material removal rate (MRR). The composite material's properties improve with the addition of graphite up to a certain percentage, beyond which they decline due to strong interfacial bonding between the particles. Furthermore, the incorporation of nickel and chromium enhances the composite material's wear resistance. Overall, the data indicates that specimens with less than 4% graphite and higher nickel-chromium content exhibit superior wear resistance compared to other reinforced compositions. Substituting the Al7075 alloy with the Al7075/Ni-Cr/graphite composite material can minimize wear and extend the material's lifespan. Future research could involve utilizing the Taguchi method in pin-on-disc testing, varying load, speed, and duration to optimize the reinforcement proportions in the base metal.

REFERENCES

1. K. K. Chawla, Composite materials: science and engineering. Springer Science & Business Media, 2012.
2. T. Trzepieciński, S. M. Najm, M. Sbayti, H. Belhadjsalah, M. Szpunar, H. G. Lemu, *J. Compos. Sci.*, **5**, 217 (2021).
3. V. Chak, H. Chattopadhyay, T. L. Dora, *J. Manuf. Process.*, **56**, 1059 (2020).
4. N. K. Singh, S. Balaguru, *Silicon*, **16**, 45 (2024).
5. N. Sreedhar, S. Balaguru, *Int. J. Mech. Prod. Eng. Res. Dev.*, **10**, 391 (2020).
6. D. Davis, G. Marappan, Y. Sivalingam, B. B.; Panigrahi, S. Singh, *ACS Omega,* **5**, 14669 (2020).
7. M. L. Parucker, A. N. Klein, C. Binder, W. Ristow Junior, R. Binder, *Mater. Res.*, **17**, 180 (2014).
8. F. Nturanabo, L. Masu, J. B. Kirabira, *Aluminum Alloys Compos.* (2019).
9. V. Madeva Nagaral, S. A. Auradi, S. V. Kori, V. Hiremath, *J. Mech. Eng. Sci.*, **13**, 4623 (2019).
10. V. Bharath, V. Auradi, S. Madeva Nagaral, S. Babu Boppana, *J. Bio- Tribo-Corros.*, **6**, 45 (2020).
11. X. Han, D. Xu, D. Axinte, Z. Liao, H. N. Li, *J. Mater. Process. Technol.*, **288**, 116875 (2021).
12. D. Palanisamy, A.; Devaraju, N.; Manikandan, K.; Balasubramanian, D. Arulkirubakaran, *Mater. Today: Proc.*, **22**, 525 (2020).
13. R. Butola, C. Pratap, A. Shukla, Walia, *Mater. Sci. Forum*, **969**, 253 (2019).
14. K. R. Padmavathi, R. Ramakrishnan, *Procedia Eng.*, **97**, 660 (2014).
15. M. V. Krishna, A. M. Xavior, *Procedia Eng.*, **97**, 918 (2014).
16. D. Das, D. K. Roy, M. P. Satpathy, B. K. Nanda, R. K. Nayak, *Mater. Today: Proc.*, **18**, 3080 (2019).

17. K. Raju, M. Balakrishnan, C. B. Priya, M. Sivachitra, D. Narasimha Rao, *Adv. Mater. Sci. Eng.* **2022**, 4438419 (2022).

18. D. Dash, S. Samanta, R. N. Rai, *Adv. Mater. Process. Technol.*, **8**, 3344 (2022).

19. R. Bobbili, V.; Madhu, A. K. Gogia, *Eng. Sci. Technol. Int. J.*, **18**, 664 (2015).

20. E. Ekici, A

21. . R. Motorcu, A. Kuş, *J. Compos. Mater.*, **50**, 2575 (2016).

22. S. Madhavarao, V. V. S. Kesava Rao, C. Rama Bhadri Raju, T. Buddi, D. V. Nemova, R. D. Nautiyal, *Cogent Eng.*, **11**, 2328822 (2024).

23. G. C. da Silva Simioni, T. D. V. Pinheiro, G. D. L. Vasques, R. V. Lantmann, M. M. Lopes, M. Wettergreen, C. A. Dos Santos, *IEEE Trans. Instrum. Meas.*, 2023.

24. R. A. Manikandan, T. V. Arjunan, *Compos. Part B Eng.*, **183**, 107668 (2020).

25. M. Sánchez, J. Rams, A. Ureña, *Compos. Part A*

Appl. Sci. Manuf., **41**, 1605 (2010).

26. J. L. Li, Y. C. Xiong, X. D. Wang, S. J. Yan, C. Yang, W. W. He, S. L. Dai, *Mater. Sci. Eng. A*, **626**, 400 (2015).

27. R. T. Yang, C. J. Tzeng, Y. K. Yang, M. H. Hsieh, *Int. J. Adv. Manuf. Technol.*, **60**, 135 (2012).

28. S. Sarkar, S. Mitra, B. Bhattacharyya, *Int. J. Adv. Manuf. Technol.*, **27**, 501 (2006).

29. M. Subrahmanyam, T. Nancharaiah, *Mater. Today: Proc.*, **23**, 642 (2020).

30. D. Chen, J. Li, K. Sun, J. Fan, *Int. J. Adv. Manuf. Technol.*, **125**, 2925 (2023).

31. K. Kumar, B. M. Dabade, L. N. Wankhade, *Mater. Today: Proc.*, **44**, 2726 (2021).

32. A. Chatterjee, S. Sen, S.; Paul, K. Ghosh, M. Ghosh, G. Sutradhar, *J. Inst. Eng. India Ser. D*, **104**, 587 (2023).

33. A. Coyal, N. Yuvaraj, R. Butola, L. Tyagi, *SN Appl. Sci.*, **2**, 1 (2020).